

<Original>

## A Study on Machine Tool Structural Dynamics by Digital Correlation Method

Jang Moo Lee\*

(Received March 12, 1981)

디지털 상관법에 의한 공작기계 구조동력학에 대한 연구

이 장 무

초 록

미니컴퓨터와 디지털 상관법을 이용하여 이상적인 아나로그 시스템의 주파수응답을 구하고 그 결과를 이론치와 비교하여 디지털 메이타 처리방법의 타당성을 검증하였다. 또한 이 방법을 실제로 복잡한 절삭중의 공작기계의 주파수응답 결정에 적용하여 이때 야기되는 문제점을 검토하고 그 해결방안을 제시하였다. 또한 제 절삭 조건하에서 얻어진 주파수응답 함수로부터 공작기계의 아머 및 시편의 길이, 절삭속도, 절삭깊이, 피이드 율에 따른 공작기계 구조동력학의 변화를 규명하였다.

### Nomenclature

$f$	: Frequency (Hz)
$f_n$	: Natural frequency (Hz)
$F(f)$	: Fourier spectrum
$H(f)$	: Transfer function
$j$	: Imaginary number
$K$	: Static gain of analogue system
$K_m$	: Stiffness of machine tool system
$n(t)$	: Noise
$N$	: Number of data
$R(\tau)$	: Correlation function
$S(f)$	: Spectral density function
$t$	: Time (sec)
$T$	: Record length of time (sec)
$x(t)$	: Input
$y(t)$	: Output

ises a cutting process and a machine tool structure. The identification of this system, which is a prerequisite for machine tool chatter analysis, is to determine the dynamic performance variables at its input. The conventional experimental method for system identification regarding dynamic rigidity of a structure is the sinusoidal sweep method (1).

However, this method has some drawbacks such as high cost, long preparation time and loading effects when the method is used for the identification of machine tool dynamics.

In recent studies, a new statistical method which was developed first in the field of communication engineering has been applied to identify the dynamics of machine tool structure under actual cutting conditions(2), (3), (4). This method, so-called correlation method, uses the inherent cutting force variation as a source of random excitation

### 1. Introduction

A machine tool system essentially compr-

\* Member, Seoul National University

without additional disturbances. The method also utilizes digital data processing and computing techniques. The rapid developments of computer hardware and software have made the techniques more powerful.

The greatest advantages of this method are time saving in experimental analysis and also possibility for the on-line control of manufacturing processes. Various instrumentation equipments and versatile data processing systems (i.e. HP 5423A signal analyzer, Spectral Dynamics SD345FFT analyzer, Nicolet Scientific Corporation 440A spectrum analyzer, etc.) thus tend to take the place of conventional experimental equipments. Limitations, however, still exist at present, such as high price of the analyzers, instrumentation noise, or fine resolution in frequency.

The objective of this study is to examine the validity and limitations of the associated instrumentation, data processing and computation algorithm by applying the method to known analogue systems and a complex machine tool system. The dynamic signals of the above systems are data-processed with a low level mini-computer, PDP11/03 which is more accessible even in poorly equipped laboratories than the special purpose signal analyzers.

## 2. The Transfer and Coherence Functions

The transfer function of a linear stationary process can be identified from its measured time series of inputs and outputs. In case of nonlinear systems the situation is more complicated. Owing to the fact that both instrumental as well as computational procedures are so complicated in the case that linearized approximations are usually made.

The method adopted here for the identification of transfer function is based on the correlation method and digital techniques. The theory of the correlation method is shown in Appendix 1. Digital techniques require that all measurements be discrete and of finite duration. Thus, this means that all continuous wave forms of the input and output data must be sampled at discrete intervals of time, uniformly separated by an interval  $\Delta t$ . Consequently, only a finite number of samples  $N$  can be taken and stored. The record length  $T$  is then

$$T = N\Delta t \quad (1)$$

The discrete values of the deviations from the mean value are processed to obtain the auto and cross correlation functions. The power and cross spectral density functions are then calculated by the discrete Fourier transform of the correlation functions. The spectral density functions can be also obtained by Fast Fourier Transform algorithm proposed by Cooley and Tukey if the number of data  $N$  is large. (5) The spectral density functions are smoothed with the Hanning's window. The transfer function estimate  $\hat{H}(f)$  is then given by,

$$\hat{H}(f) = \frac{\hat{S}_{xy}(f)}{\hat{S}_x(f)} \quad (2)$$

where denotes the estimated values. As a measure of the accuracy (noise and/or non-linear effects) of the estimation, coherence function  $\hat{r}(f)$  is defined by

$$\hat{r}^2(f) = \frac{|\hat{S}_{xy}(f)|^2}{\hat{S}_x(f) \cdot \hat{S}_y(f)} \quad \text{where } 0 \leq \hat{r}^2 \leq 1.$$

Detail calculation procedures for the spectral density function estimates,  $\hat{S}_x(f)$ ,  $\hat{S}_y(f)$  and  $\hat{S}_{xy}(f)$  are shown in Appendix 2 and the associated computer program package can be found from the author's previous work (6). As a result of discrete data process, the

spectral density function estimates are obtained at discrete frequencies and with finite resolution up to a maximum frequency,  $f_{max}$ , which according to Shannon's sampling theorem, obeys

$$f_{max} = \frac{1}{2\Delta t} \tag{4}$$

Thus, the maximum frequency resolution  $\Delta f$  obtainable for a sampled record of length,  $T$ , becomes

$$\Delta f = \frac{1}{T} \tag{5}$$

Also important in the digital data processing technique is the ensemble averaging. (7). In the real world as in the measurement of transfer function of a complex machine tool system, signals of interest are often obscured by the presence of noise. Noise in many cases, however, is known to be random and independent of signals of interest. If we thus take repeated time or frequency records of noisy signals, and average these records, some portion of the noise will average to zero (if enough averages are taken) and the previously hidden signal will be enhanced. It is because of the above that computation of spectra and transfer function was carried out with averaging in this study. In the measurement system of this study, two types of noise, system noise  $n(t)$  and instrumentation noise  $n_1(t)$  and  $n_2(t)$ , exist as shown in Fig. 1.

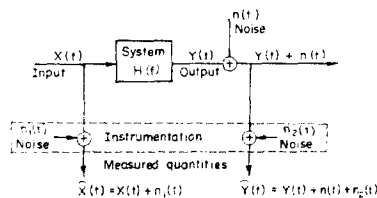


Fig. 1 System with consideration of noise.

The spectral density and transfer function

of the system with noise,  $S_{xn}(f)$ ,  $S_{xyn}(f)$  and  $H_n(f)$  can be expressed in terms of Fourier spectra,  $F_x(f)$ ,  $F_y(f)$ ,  $F_n(f)$ ,  $F_{n1}(f)$  and  $F_{n2}(f)$  as follows:

$$S_{xn}(f) = F_x(f) F_x^*(f) + F_x(f) F_{n1}^*(f) + F_x^*(f) F_{n1}(f) + F_{n1}(f) F_{n1}^*(f) \tag{6}$$

$$S_{xyn}(f) = H(f) F_x(f) F_x^*(f) + H(f) F_x(f) F_{n1}^*(f) + F_n(f) F_x^*(f) + F_n(f) F_{n1}^*(f) + F_{n2}(f) F_x^*(f) + F_{n2}(f) F_{n1}^*(f) \tag{7}$$

$$H_n(f) = \frac{S_{xyn}(f)}{S_{xn}(f)} \tag{8}$$

Thus, if the noise is random and independent of the signals, the averaged transfer function  $[H_n(f)]_{averaged}$  becomes

$$[H_n(f)]_{averaged} = \frac{[S_{xyn}(f)]_{averaged}}{[S_{xn}(f)]_{averaged}} = \frac{H(f) + \frac{F_{n2}(f) F_{n1}^*(f)}{S_x(f)}}{1 + \frac{|F_{n1}(f)|^2}{S_x(f)}} \tag{9}$$

### 3. Experiments

#### 3.1. Experimental Procedure for Analogue System.

Random tests were carried out to identify the transfer functions of known analogue systems and thus to confirm the validity of the digital data processing procedure employed in this study. In addition, by comparing the test results of analogue systems with those of real complex machine tool systems, significant source of instrumentation error can be identified. For this purpose two linear systems of the following response functions were constructed on an analogue computer (Hitachi, ALS 20n). Its analogue circuit design is shown in Fig. 2.

$$H_1(f) = \frac{63,000}{(2\pi f)^2 + 60(2\pi f) + 63,000} \tag{10}$$

where the natural frequency  $f_n = 40\text{Hz}$ , static

gain  $K=1.0$  and damping ratio  $\zeta=0.125$

$$H_2(f) = \frac{474,000}{(2\pi f)^2 + 125(2\pi f) + 1,580,000} \quad (11)$$

where  $f_n=200\text{Hz}$ ,  $K=3.33$  and  $\zeta=0.05$ .

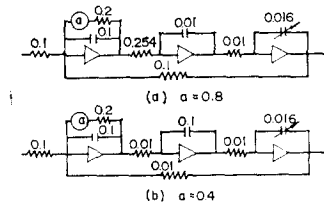


**Fig. 2** Analogue circuits of known systems.  
(a)  $H_1(f)$  (b)  $H_2(f)$

White random noise from a random noise generator (Rion Company) was used as a system input signal to ensure enough variety of frequency components, and the noise was pre-filtered with low pass filter (NF circuit Design Block Co., FV-606T) at the cut-off frequency of 500Hz to avoid aliasing error due to the digital sampling rate of 1000/sec. The decay rate of the low pass filter beyond the cut-off frequency was 36 dB/oct and the signal to noise ratio (S/N) at a nominal input level (3V rms) was more than 70 dB. Also the distortion in frequency range 20 Hz- 20 KHz was below 1%. This pre-filtered signal was fed into the pre-designed analogue circuits to yield system output signal. Drifts of the operational amplifiers of the analogue computer were less than  $\pm 3.0\mu\text{V}/^\circ\text{C}$ . Inaccuracy in resistance and capacitance was less than  $\pm 0.05\%$ . In order to check the stationarity of the input and output signal, the mean and rms values of the signals were measured with a probability analyzer (Kanomax SAI-42A) for different time origins and averaging time. As can be expected, the variation of mean and rms values was negligibly small. Both the input and output were recorded on a data recorder (Shinkoh,

9101) for digital data processing.

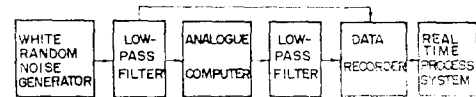


**Fig. 3-** A schematic diagram of the experimental set-up of the analogue systems.

### 3.2. Experimental Procedure for a Machine Tool Structure.

Random tests were carried out with a productive high speed lathe (Okuma, LS 450) to determine machine tool structural dynamics at the cutting point under various cutting conditions. The random input and output of the system to be used are the thrust force component and the corresponding tool workpiece relative displacement. A schematic illustration of the test set-up is shown in Fig. 4.

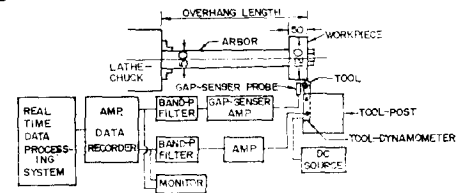


**Fig. 4** A schematic diagram of the experimental set-up of the machine tool structure.

A disk-like workpiece prepared from SF-45 steel rod was turned with longitudinal feed. A tool (Sandvix, R181, 3-2020-12) with carbide TA type tip (SNMG 20) was used. As shown in Fig. 5, the tool-workpiece relative displacement during cutting was measured by an eddy current type gap sensor which consists of a pick-up (PU-05) and an amplifier (AEC-2525-05). The sensitivity of the pick-up was  $5\text{mV}/\mu$ . In order to measure the thrust cutting force variation without influencing the cutting system, the lowest natural frequency of tool-dynamometer should be more than 2 or 3 times as large as the significant natural frequencies of the

cutting system. A preliminary, simple impulse test was carried out with the tool tip firmly contacting the static workpiece. The highest, significant natural frequency of the system was found to be 417 Hz. Since the natural frequency of the heavy conventional tool-dynamometer (such as Mituho Electric's AST) was about 500Hz, a specially designed tool dynamometer was home-fabricated as shown in Fig. 6. The natural frequency of the tool-dynamometer was found to be 1050Hz. The sensitivity of the tool dynamometer with dynamic strain amplifier (S.N. U. F.I.C.) was 2.3mV/Kg. By using two identical FV-606 filter, the signals are high-pass filtered with cut-off frequency being 2Hz to eliminate DC component and low-pass filtered with cut-off frequency being 500Hz to avoid aliasing since the sampling rate was set at 1000/sec. The signals were then amplified to a full scale range of about  $\pm 1V$  with a DC amplifier (SAN-EI Type 6L3-1) and stored in the data recorder for digital data processing.

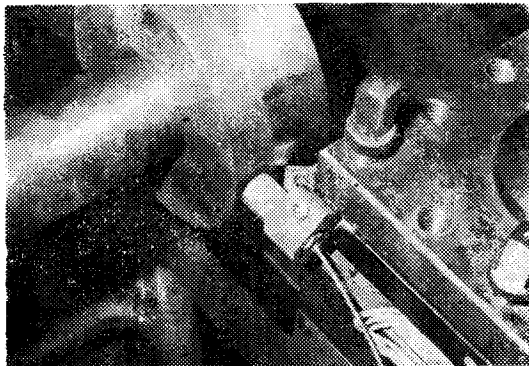


**Fig. 5** Experimental set-up for the measurement of displacement.

In order to investigate the variation on machine tool structural dynamics, cutting conditions are selected as shown in Table 1. By doing this way, three different conditions are obtained respectively for the change of

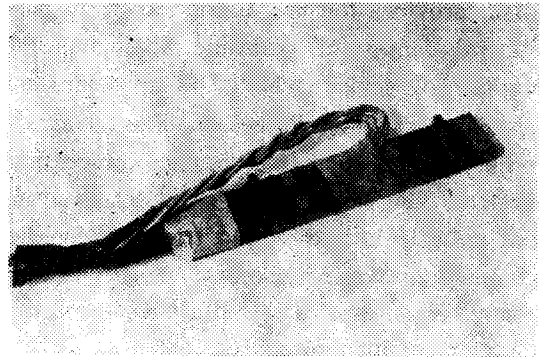


**Fig. 6** Home-fabricated tool dynamometer.

overhang length of the arbor, cutting speed, depth of cut and feed rate. More than 20 ensembles of input and output signals were stored in the data recorder for each cutting conditions. Also, the stationarity of the input and output signals was checked out and will be discussed later.

**Table 1** Cutting conditions.

Test case NO.	Overhang length (mm)	Cutting speed (m/min)	Depth of cut (mm)	Feed rate (mm/rev)
1	100	45	0.2	0.10
2	150	24	0.2	0.10
3	150	45	0.2	0.10
4	150	80	0.2	0.10
5	150	45	0.5	0.10
6	150	45	1.0	0.10
7	150	45	0.2	0.05
8	150	45	0.2	0.15
9	175	45	0.2	0.10

### 3.3. Data Processing Procedures

The data processing was carried out using PDP-11/03 minicomputer (CPU core memory; 32KW, floppy disk; 128KW). The PDP-11/03 system which is operated by the RT-11 FORTRAN operating system contains the DECLAB-03 FORTRAN SYSTEM and the DECLAB-03 FORTRAN extensions. The LSILIB library which is included as an object file on the DECLAB-03 FORTRAN system

disk, provides the use of the hardware peripheral family of real-time analogue and digital I/O devices which DEC provides as options for LSI-11 Processor. The data recorder is connected to the data processing system. The sampling rate was set at 1000/sec and calculations were carried out by the computer program package developed in this study. Fig. 7 shows the illustration of the data processing procedures.

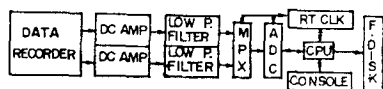


Fig. 7 Data processing produres.

#### 4. Results and Discussions

The computer program developed for the digital data processing in this study was executed to obtain the correlation, spectral density and transfer functions of both the analogue systems and the machine tool structure. Fig. 8 shows the typical outputs of correlation and spectral density function for an analogue system ( $f_n=200\text{Hz}$ ). The following observation can be made from the theoretical point of view. The autocorreltaion of input reveals delta function nature and the power-spectrum of input reveals constant spectrum nature since the input was approximately white-noise. Also, the auto-correlation of output reveals damped oscillatory nature and the power-spectrum of output reveals single sharp peak nature since the analogue system was lightly damped system of single degree of freedom (i.e. the output was a narrow frequency-band random signal). Experimentally obtained transfer functions of the analogue systems are compared with the theoretically calculated transfer functions in Fig. 9 and Fig. 10. The results show that

the experimental values agree well with the theoretical results. This fact indicates that the data processing procedures used in this study were valid.

However, in practical situations such the identification of transfer function of a machine tool system, some experimental difficulties were observed particularly in connection with noise. The first difficulty comes from the non-linearity of the machine tool system under cutting. In other words, if the cutting condition such as input force level changes, the natural frequency and damping will change. Thus machine tool dynamics should be obtained for each cutting condition and the dynamics thus obtained is considered to be valid only near the particular cutting condition. In order to check the linearity of the machine tool system, the first order (amplitude) probability density functions of the input force and the output tool-workpiece

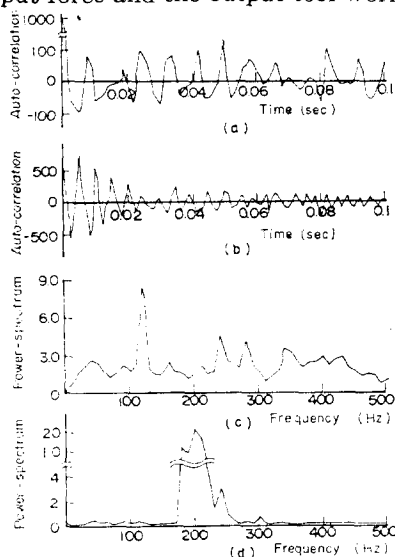
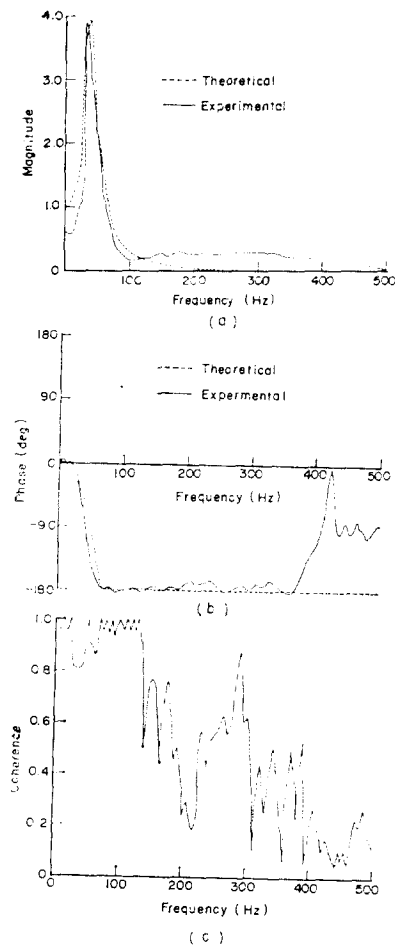


Fig. 8 The correlation and spectral density functions of an analogue system ( $f_n=200\text{Hz}$ ).

(a) Auto-correlation of input.  
 (b) Auto-correlation of output.  
 (c) Power-spectral density of input.  
 (d) Power-spectral density of output.



**Fig. 9** Transfer function of an analogue system ( $f_n=40\text{Hz}$ ).

(a) magnitude (b) phase (c) coherence

relative displacement signals were measured by use of the probability analyzer. The probability density plots shown in Fig. 11 indicate that the probability function of input closely resembles Gaussian distribution while that of output slightly deviates from Gaussian distribution. It is well known that this kind of system behavior can be easily observed from a system containing non-linear stiffness element of the hardening spring type (8). This behavior tends to be more remarkable as the cutting condition become

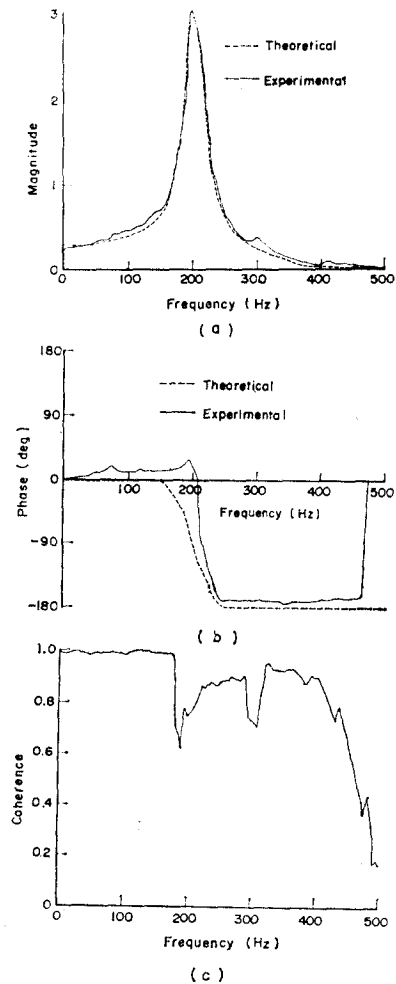


**Fig. 10** Transfer function of an analogue system ( $f_n=200\text{Hz}$ ).

(a) magnitude (b) phase (c) coherence

more severe (i.e., the amplitude of vibration become larger). The second difficulty arises from the system and instrumentation noise as mentioned before. In this study, system noise  $n(t)$  was found to be mainly due to the surface roughness and unbalanced rotation of the workpiece.

The input instrumentation noise  $n_1(t)$  was the most serious obstacle when the extreme care was not taken of shielding, grounding, wiring and amplifying. As mentioned before,

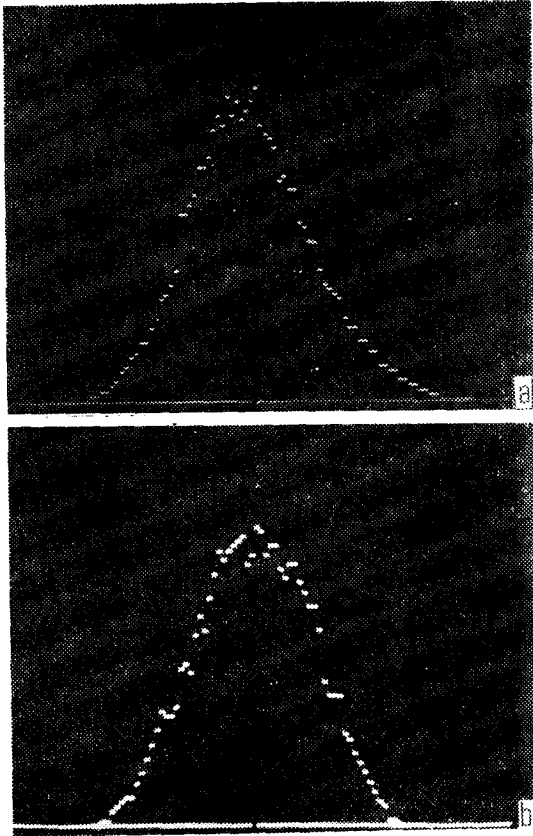


**Fig. 11** Probability density plots of input (a) and output (b) signals (cutting speed : 24m/min, overhang : 150mm, depth of cut : 0.5mm, feed rate : 0.10mm/rev)

the natural frequency of the tool dynamometer should be sufficiently higher than the significant frequencies of the machine tool system. Since the high natural frequency and consequently the high stiffness of the tool dynamometer can be achieved at the cost of sensitivity (gain), low noise (especially without 60Hz noise) strain amplifier and high gain (up to 5000 times) DC amplifier had to be used. On the other hand, the output instrumentation noise  $n_2(t)$  was negligibly small. However, the distortion of the probability distribution was also partially

due to the system noise  $n(t)$ . Signal to noise ratio in this experiment was greater than 10. The third difficulty came from the fact that input force spectrum of machine tool system did not contain enough energy over wide frequency range of the machine tool system. For this reason comparatively high coherence function was obtained in the frequency region near the natural frequency.

Since the statistical properties (such as mean and variance) of the cutting process in this study varied slightly with time, the processes were approximately stationary. Thus ensemble averages were taken over 20 repeated samplings.

Fig. 12 shows transfer functions and coherence functions of the machine tool system of cutting point by single measurement and ensemble averaged measurement. As expected, the coherence becomes better for averaged measurement than single measurement. It can be also noted that phase change of 180 degree occurs near natural frequency.

Other transfer functions of the machine tool system at cutting point for various cutting conditions were obtained in the same manners. Generally, the largest resonance peaks were observed over the frequency range of 260Hz~340Hz while the resonance occurred at 417Hz under static condition (without cutting). This fact indicates that the natural frequencies of the machine tool system at cutting point (mainly due to arbor and workpiece) change depending on the cutting conditions and consequently the use of transfer function data obtained without cutting will cause enormous error in chatter analysis. The resonance peaks were also observed near 12Hz and 150Hz. For convenience, the transfer functions of machine tool system at cutting point may be regarded as



those of a single degree of freedom system with natural frequencies at 260Hz~340Hz. Then the damping ratio  $\zeta$  and the static stiffness  $K_n$  can be calculated from the 3dB frequency band-width  $\Delta f$ , natural frequency  $f_n$  and the maximum transfer function gain  $H_{\max}$  (9), as shown in Fig. 13. The results thus obtained are summarized in Table 2. From the transfer function data obtained for different values of overhang length of arbor, cutting speed, depth of cut and feed rate, the following observations can be made.

As can be seen from Table 2, there is no consistent trend in transfer function for the change in cutting speed. The natural frequencies of the transfer functions were 271Hz for the cutting speeds of 24m/min (revolutions of main spindle, 63 rpm) and 264Hz for the cutting speeds of both 45m/min and 80m/min. The damping ratios were about 0.04 and the static stiffness were 1.22~1.31 kg/ $\mu$ .

As can be seen from Table 2, the natural frequency increases from 264Hz and 280Hz and the damping ratio increases from 0.042 to 0.054 when the depth of cut changes from 0.2mm to 0.5mm and 1.0mm. This is due to the fact that as the depth of cut become larger, the tool tip presses the free end of the arbor (workpiece) harder and the stiffness of the arbor becomes larger as in the hardening spring. Thus the static stiffness increased from 1.3Kg/ $\mu$  to 1.38Kg/ $\mu$  and 1.54Kg/ $\mu$ .

As can be seen from Table 2, the natural frequency decreases from 338Hz to 264Hz and 253Hz, the damping ratio decreases from 0.055 to 0.042 and 0.030, and the static stiffness decreases from 1.85Kg/ $\mu$  to 1.31 Kg/ $\mu$  and 0.94Kg/ $\mu$  when the overhang length of the arbor increases from 100mm

to 150mm and 175mm. The results can be intuitively expected since the larger the length of bar is, the lower the flexural natural frequency is. It was also observed that when the arbor (workpiece) is extremely short (100mm), other resonance peaks near 12Hz and 125Hz become comparable to that of arbor and workpiece. From the supplementary test results, it is suspected that 10Hz is due to machine tool-foundation interaction and 125Hz is due to main spindle.

As can be seen from Table 2, there is no

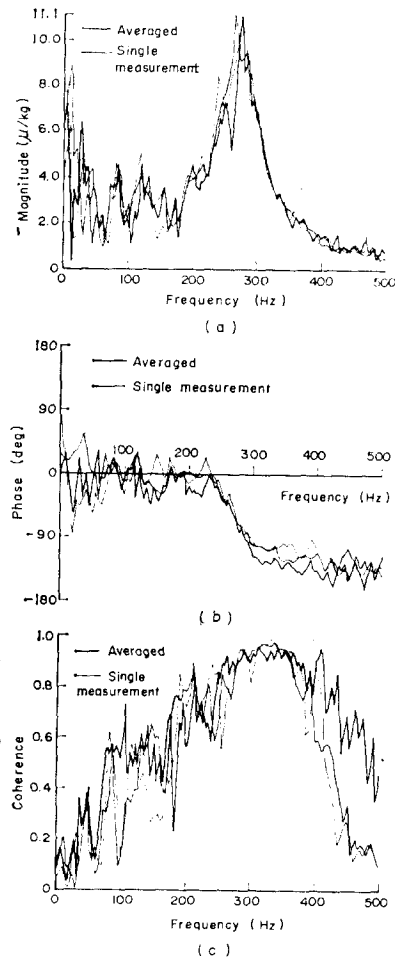


Fig. 12 Magnitude (a) and phase (b) of the transfer function and coherence function (c) of the machine tool system. (test case No. 2).

**Table 2** Parameters of the transfer function of the machine tool under various cutting conditions.

Variable	Condition	Test case NO.	$f_n$ (Hz)	$\zeta$	$K_m$ (Kg/ $\mu$ )
Cutting speed	24m/min	2	271	0.037	1.22
	45m/min	3	264	0.042	1.31
	80m/min	4	264	0.034	1.23
Depth of cut	0.2mm	3	264	0.042	1.31
	0.5mm	5	277	0.042	1.38
	1.0mm	6	280	0.054	1.54
Overhauling length	100mm	1	338	0.055	1.85
	150mm	3	264	0.042	1.31
	175mm	9	253	0.030	0.94
Feed rate	0.05mm/rev	7	278	0.045	1.25
	0.10mm/rev	3	264	0.042	1.31
	0.15mm/rev	8	299	0.042	1.37

consistent trend in transfer function for the change in feed rate. The natural frequency of the arbor and workpiece changes from 278Hz to 264Hz and 299Hz, the damping ratio remains constant at about 0.04 and the static stiffness increases from 1.25Kg/ $\mu$  to

1.31Kg/ $\mu$  and 1.37Kg/ $\mu$  as the feed rate changes from 0.05mm/rev to 0.10mm/rev and 0.15mm/rev. As in the depth of cut, increase in the feed rate cause larger compressive force to the arbor and workpiece and may contribute to the increase of natural frequency. However, the natural frequency increased slightly also at lower feed rate.

## 5. Conclusions

In this study, the transfer functions of the ideal analogue systems and the complex machine tool system at cutting point were obtained by using digital correlation method. The different features of the analogue and machine tool systems identification were discussed. Also the variations of machine tool dynamics under various cutting conditions were investigated and the following observations were made:

- 1) No consistent trend in transfer function is observed for the change in cutting speed.
- 2) Increase in the depth of cut causes increase in the natural frequency and damping.
- 3) Increase in the length of arbor causes decrease in the natural frequency and damping.
- 4) No consistent trend in transfer function is observed for the change in feed rate.
- 5) The natural frequency of the machine tool system at cutting point was 417Hz under static condition and 260Hz~340Hz under actual cutting conditions. Thus the former can not be safely used in chatter analysis.

## Acknowledgements.

This work was supported by a financial

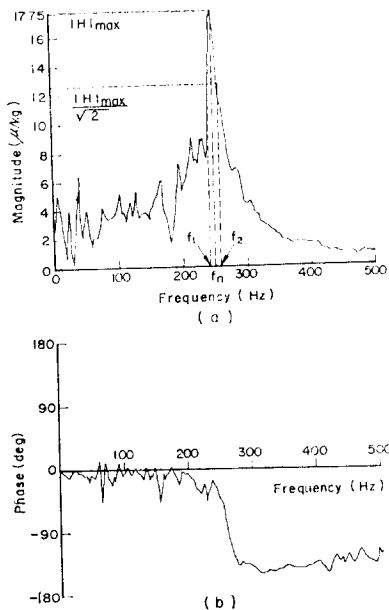


**Fig. 13** Magnitude (a) and phase (b) of the transfer function of the machine tool system. (test case No. 9),

aid of the 1979 Korea Science and Engineering Foundation Grant. The author wishes to thank to Mr. Myun Chul Kim, Mr. Jun Kyo Suh and Mr. Seung Jin Huh for their assistance in this study.

**Appendix 1.** Theory of the Correlation Method

Consider a single input-output linear system with an impulse response function  $h(\tau)$  and frequency response function  $H(f)$ .

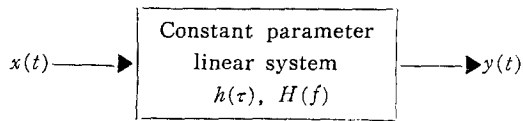


**Fig. A-1** Single input-output linear system.

In Fig. A-1,  $x(t)$  and  $y(t)$  are input and output of the system respectively which belong to stationary random processes transformed to have zero mean values. The auto-correlation function  $R_x(\tau)$  is defined as (3)

$$R_x(\tau) = E[x(t) \cdot x(t+\tau)] \\ = \lim_{t \rightarrow \infty} \frac{1}{t} \int_0^t x(t) \cdot x(t+\tau) dt. \quad (A-1)$$

Fourier transform of the auto-correlation function

$$S_x(f) = \int_{-\infty}^{\infty} R_x(\tau) \exp(-j2\pi f\tau) d\tau, \\ -\infty < f < \infty \quad (A-2)$$

where  $f$  is the frequency, gives the two-sided power spectral density function. The cross-correlation function between the input  $x(t)$  and the output  $y(t)$  is also expressed as

$$R_{xy}(\tau) = E[x(t) \cdot y(t+\tau)] \\ = \lim_{t \rightarrow \infty} \frac{1}{t} \int_0^t x(t) \cdot y(t+\tau) dt \quad (A-3)$$

and two-sided cross-spectral density function  $S_{xy}(f)$  is given by

$$S_{xy}(f) = \int_{-\infty}^{\infty} R_{xy}(\tau) \exp(-j2\pi f\tau) d\tau, \\ -\infty < f < \infty \quad (A-4)$$

From Fig. A-1 the output  $y(t)$  can be expressed as a convolution of input  $x(t)$ , that is,

$$y(t) = \int_0^{\infty} h(\tau) \cdot x(t-\tau) d\tau \quad (A-5)$$

Through some mathematical manipulation with above equations, the following relationships are obtained:

$$R_y(\tau) = \int_0^{\infty} \int_0^{\infty} h(\xi) h(\eta) R_x(\tau+\xi-\eta) d\xi d\eta \quad (A-6)$$

$$R_{xy}(\tau) = \int_0^{\infty} h(\xi) R_x(\tau-\xi) d\xi \quad (A-7)$$

The transformation of equations (A-6) and (A-7) into a complex-valued frequency domain by taking Fourier transforms yields

$$S_y(f) = |H(f)|^2 \cdot S_x(f) \quad (A-8)$$

$$S_{xy}(f) = H(f) \cdot S_x(f) \quad (A-9)$$

**Appendix 2.** Digital Computation Method of the Correlation and Spectral Density Functions.

The correlation and spectral density functions are calculated in the following manner when the input  $x(t)$  and the output  $y(t)$  are sampled at a constant interval  $dt$ . Denoting the sampled value of  $x(t)$  at time  $t=kdt$  ( $k=1, 2, \dots, N$ ) by  $X(K)$ , the following relationships are obtained.

$$R_x(i) = \frac{1}{N} \sum_{n=1}^{N-i} [X(i+n) - \bar{X}][X(n) - \bar{X}] \\ \text{for } i=0, 1, 2, \dots, h. \quad (A-10)$$

$$R_{xy}(i) = \frac{1}{N} \sum_{n=1}^{N-i} [Y(i+n) - \bar{Y}][X(n) - \bar{X}] \\ \text{for } i=0, 1, 2, \dots, h. \quad (A-11)$$

$$R_{xy}(i) = \frac{1}{N} \sum_{n=1-i}^N [Y(i+n) - \bar{Y}][X(n) - \bar{X}] \\ \text{for } i=-1, -2, \dots, -h. \quad (A-12)$$

$$\bar{X} = \frac{1}{N} \sum_{n=1}^N X(n) \quad (A-13)$$

$$\bar{Y} = \frac{1}{N} \sum_{n=1}^N Y(n) \quad (\text{A-14})$$

$$S_x(r) = \Delta t \{ R_x(0) + 2 \sum_{i=1}^{h-1} \cos(\pi \frac{r}{h} i) R_x(i) \\ + (-1)^r R_x(h) \} \quad (\text{A-15})$$

for  $r=0, 1, 2, \dots, h$ .

$$S_{xy}(r) = \sum_{i=-h}^h \exp(-j\pi \frac{r}{h} i) R_{xy}(i) \Delta t \quad (\text{A-16})$$

for  $r=-h, -h+1, \dots, h-1, h$ .

$$S_x(r) = \sum_{m=-2}^2 W(m) S_x(r-m) \quad (\text{A-17})$$

$$S_{xy}(r) = \sum_{m=-2}^2 W(m) S_{xy}(r-m) \quad (\text{A-18})$$

where  $W(m)$  is Hanning's window function.

### References

1. C.M. Harris and C.E. Crede, Shock and Vibration Handbook, McGraw-Hill 1961
2. A.W. Kwiatkowski and F.E. Bennet, "Correlation Method of System Identification Computer Programme and Experiment Design Considerations", Proc. of 7th Int. M.T.D.R. Conf. 1966
3. Myun Chul Kim, "A Study on the Computer-Implemented Analysis of Machine Tool Vibration", M.S. Thesis, Seoul National University, 1979
4. Jun Kyo Suh, "A Study on the Machine Tool Structural Dynamics by Using Mini-computer", M.S. Thesis, Seoul National Univ., 1980
5. J.S. Bendat and A.G. Piersol, "Random Data Analysis and Measurement Procedures", Wiley-Interscience, 1971
6. J.M. Lee, R. Lee, D.W. Kim, M.C. Kim and K.J. Kim, "Optimization of the Dynamic Characteristics of Machine Tools", Policy Project of Ministry of Education, 1977
7. K.A. Ramsey, "Effective Measurements for Structural Dynamics Testing", Sound and Vibration, 1975
8. S.H. Crandall, "Random Vibration of a Non-linear System with Set-up Spring." Journal of Applied Mechanics. Vol. 20, 1962
9. F.S. Tse, I.E. Morse and R.T. Hinkle, "Mechanical Vibrations", Allyn and Bacon, Inc., 1978
10. T. Moriwaki and T. Hoshi, "System Identification on Digital Techniques-New Tools for Dynamic Analysis", Keynote paper for the 24th General Assembly of C.I.R.P., 1974